

A Family of Hyperbolic and Exponential–Type Controllers

Francisco Terneus , Fernando Reyes and Eduardo Lebano

Abstract—This paper addresses the problem of position control for robot manipulators. A new family of controllers with gravity compensation for the global position is presented. This new family called Hyperbolic controller has its structure composed by exponential hyperbolic functions, that force the position error to move to zero position. This paper offers enough conditions that are sufficient in order to prove directly global asymptotic stability of the closed-loop system composed by the nonlinear robot dynamics for n degrees of freedom and the proposed scheme. In addition to the theoretical results, real-time experiments are presented to compare the performance of the proposed family with other well-known control algorithms such as the PD on a three degrees of freedom direct-drive robot arm.

Keywords—Global asymptotic stability, Lyapunov function, PD controller, robot manipulators, position control.

I. INTRODUCTION

POSITION control, otherwise known as the so-called regulation problem is one of the most relevant issues in the practice of manipulators. This is a particular case of the trajectory control. Regulation has attracted a considerable amount of attention (see [1] and the references cited therein). It is based on moving the manipulator from any initial state to a fixed desired configuration [2] [3]. The problem of designing regulators is ensuring asymptotic position error and joint velocity to zero. Regulators that achieve this objective for all desired targets and all initial conditions are said to be globally convergent [4].

Lyapunov functions are an indispensable tool in analysis and design of controllers for nonlinear systems and play an important role in the stability study of robot manipulators. The asymptotic stability is achieved using the LaSalle invariance principle [5].

We use the methodology by energy shaping plus damping injection technique introduced by Takegaki and Arimoto[6] to study the simple PD control with gravity compensation, considered a landmark in robot control. Using energy shaping it yields a global stable closed-loop system for a trivial selection of proportional and derivative gains, and by applying LaSalle's invariance principle the asymptotic stability is achieved [7]. Many authors have used energy shaping to design control schemes using a weak Lyapunov function [8] — [10].

They obtain a global stable closed-loop system. The global

asymptotic stability is obtained with LaSalle's invariance principle [11] — [16].

In view of the simplicity and applicability of the simple PD controller in industrial applications, the purpose of this paper is to unify the previous results of the linear PD control on a large class of Hyperbolic-type controllers for robot manipulators that lead to global asymptotic stability of the closed-loop system (dynamics model of robot manipulator plus controller) by using the direct method of Lyapunov. The proposed control scheme has a nonlinear structure, which incorporates components of hyperbolic type to quickly drive the position error to zero position. In addition to the theoretical issues of the proposed family; this paper also presents a real-time comparative study of four position controllers : three membership controllers of the proposed family vs. the PD controller on a three degrees of freedom direct-drive arm.

This paper is organized as follows. Section 2 recalls the robot dynamics and useful properties for stability proof. In Section 3, the proposed hyperbolic family is presented and its analysis of global asymptotic stability with a Lyapunov function. Section 4 summarizes the main components of the experimental set-up. Section 5 contains the experimental comparison with three controllers of the proposed family vs the PD controller on a three degrees of freedom arm. Finally, some conclusions are offered in Section 6.

II. ROBOT DYNAMICS

In the absence of friction phenomena and other disturbances, the dynamics of a serial n -link rigid robot [17] can be written as:

$$M(\mathbf{q})\ddot{\mathbf{q}} + C(\mathbf{q}, \dot{\mathbf{q}})\dot{\mathbf{q}} + \mathbf{g}(\mathbf{q}) = \boldsymbol{\tau} \quad (1)$$

where \mathbf{q} is the $n \times 1$ vector of joint displacements, $\dot{\mathbf{q}}$ is the $n \times 1$ vector of joint velocities, $\boldsymbol{\tau}$ is the $n \times 1$ vector of input torques, $M(\mathbf{q})$ is the $n \times n$ symmetric positive definite manipulator inertia matrix, $C(\mathbf{q}, \dot{\mathbf{q}})$ is the $n \times n$ matrix of centripetal and Coriolis torques, and $\mathbf{g}(\mathbf{q})$ is the $n \times 1$ vector of gravitational torques obtained as the gradient of the robot potential energy due to gravity.

It is assumed that the robot links are joined together with revolute joints. Although the equation of motion (1) is complex, it has several fundamental properties which can be exploited to facilitate control system design. For the proposed controller, the following important properties are used:

Property 1. The inertia matrix $M(\mathbf{q})$ is a symmetric, positive definite, therefore $\exists M(\mathbf{q})^{-1}$ and it is also a symmetric, positive definite matrix. Both $M(\mathbf{q})$ and $M(\mathbf{q})^{-1}$ are uniformly

Work partially supported by CONACYT 91503, México
Francisco Terneus is part of The Universidad Popular Autónoma del Estado de Puebla, Puebla, México
and Escuela Superior Politécnica del Ejército, Quito, Ecuador. email: pacoterneus@hotmail.com
Fernando Reyes is part of Grupo de Robótica, Benemérita Universidad Autónoma de Puebla, Puebla,
México, Apartado Postal 542, Puebla 72001, México, Tel/Fax: +(52) 222 2 29 55 00 ext. 7410, email:
freyes@ece.buap.mx
Eduardo Lebano is part of the Universidad Popular Autónoma del Estado de Puebla, Puebla, México

bounded as a function of $\mathbf{q} \in \mathbb{R}^n$, this is $\|M(\mathbf{q})\| < \beta$, where β is a positive real constant, strictly speaking, boundedness of the inertia matrix requires in general, that all joints be revolute:[18] [19]

$$\beta \geq n(\max_{i,j} |M_{ij}(\mathbf{q})|)$$

where M_{ij} are elements of $M(\mathbf{q})$.

Property 2. See Koditschek[18] Spong & Vidyasagar[17] and Romeo *et al.* [19] the matrix $C(\mathbf{q}, \dot{\mathbf{q}})$ defined using the Christoffel symbols and the time derivative $\dot{M}(\mathbf{q})$ of the inertia matrix satisfy:

1. $\dot{\mathbf{q}}^T \left[\frac{1}{2} \dot{M}(\mathbf{q}) - C(\mathbf{q}, \dot{\mathbf{q}}) \right] \dot{\mathbf{q}} = \mathbf{0} \quad \forall \mathbf{q}, \dot{\mathbf{q}} \in \mathbb{R}^n$.
2. $\dot{M}(\mathbf{q}) = C(\mathbf{q}, \dot{\mathbf{q}}) + C(\mathbf{q}, \dot{\mathbf{q}})^T \quad \forall \mathbf{q}, \dot{\mathbf{q}} \in \mathbb{R}^n$.

Property 3. The Coriolis matrix $C(\mathbf{q}, \dot{\mathbf{q}})$ satisfies the following:[17] [19]

1. If $\dot{\mathbf{q}} = \mathbf{0}$ then $C(\mathbf{q}, \dot{\mathbf{q}}) = \mathbf{0} \in \mathbb{R}^{n \times n} \quad \forall \mathbf{q} \in \mathbb{R}^n$.
2. $\dot{\mathbf{q}}^T C(\mathbf{q}, \dot{\mathbf{q}}) \dot{\mathbf{q}}$ is bounded as a function of $\mathbf{q}, \dot{\mathbf{q}} \in \mathbb{R}^n$, then $\|\dot{\mathbf{q}}^T C(\mathbf{q}, \dot{\mathbf{q}}) \dot{\mathbf{q}}\| < \|\dot{\mathbf{q}}\|^2 k_c$, where $k_c \in \mathbb{R}_+$.

III. A FAMILY OF HYPERBOLIC AND EXPONENTIAL-TYPE CONTROLLERS

This section presents the proposed hyperbolic and exponential family of controllers and its global asymptotic stability analysis. We intend to extend the results on the simple PD controller to a large class of hyperbolic-type controllers for robot manipulators. Consider the following control scheme with gravity compensation given by

$$\begin{aligned} \boldsymbol{\tau} = & K_p \frac{sh(\lambda \tilde{\mathbf{q}})(1 - e^{-ch(\lambda \tilde{\mathbf{q}})})}{ch(\lambda \tilde{\mathbf{q}}) + e^{-ch(\lambda \tilde{\mathbf{q}})}} \\ & - K_v \frac{sh(\alpha \dot{\tilde{\mathbf{q}}})(1 - e^{-ch(\alpha \dot{\tilde{\mathbf{q}}})})}{ch(\alpha \dot{\tilde{\mathbf{q}}}) + e^{-ch(\alpha \dot{\tilde{\mathbf{q}}})}} + \mathbf{g}(\mathbf{q}) \end{aligned} \quad (2)$$

where $K_p \in \mathbb{R}^{n \times n}$ is the proportional gain which is a diagonal matrix, $K_v \in \mathbb{R}^{n \times n}$ is a positive definite matrix, so-called derivative gain, and the following terms are defined as:

$$\frac{sh(\lambda \tilde{\mathbf{q}})(1 - e^{-ch(\lambda \tilde{\mathbf{q}})})}{ch(\lambda \tilde{\mathbf{q}}) + e^{-ch(\lambda \tilde{\mathbf{q}})}} = \begin{bmatrix} \frac{sh(\lambda_1 \tilde{q}_1)(1 - e^{-ch(\lambda_1 \tilde{q}_1)})}{ch(\lambda_1 \tilde{q}_1) + e^{-ch(\lambda_1 \tilde{q}_1)}} \\ \vdots \\ \frac{sh(\lambda_n \tilde{q}_n)(1 - e^{-ch(\lambda_n \tilde{q}_n)})}{ch(\lambda_n \tilde{q}_n) + e^{-ch(\lambda_n \tilde{q}_n)}} \end{bmatrix} \quad (3)$$

$$\frac{sh(\alpha \dot{\tilde{\mathbf{q}}})(1 - e^{-ch(\alpha \dot{\tilde{\mathbf{q}}})})}{ch(\alpha \dot{\tilde{\mathbf{q}}}) + e^{-ch(\alpha \dot{\tilde{\mathbf{q}}})}} = \begin{bmatrix} \frac{sh(\alpha_1 \dot{\tilde{q}}_1)(1 - e^{-ch(\alpha_1 \dot{\tilde{q}}_1)})}{ch(\alpha_1 \dot{\tilde{q}}_1) + e^{-ch(\alpha_1 \dot{\tilde{q}}_1)}} \\ \vdots \\ \frac{sh(\alpha_n \dot{\tilde{q}}_n)(1 - e^{-ch(\alpha_n \dot{\tilde{q}}_n)})}{ch(\alpha_n \dot{\tilde{q}}_n) + e^{-ch(\alpha_n \dot{\tilde{q}}_n)}} \end{bmatrix} \quad (4)$$

where λ_i and $\alpha_i \in \mathbb{R}_+$, $\tilde{\mathbf{q}} \in \mathbb{R}^n$ is the position error vector, which is defined as $\tilde{\mathbf{q}} = \mathbf{q}_d - \mathbf{q}$, where $\mathbf{q}_d \in \mathbb{R}^n$ represents the desired joint position; ch() and sh() are the hyperbolic cosine and sine functions respectively and e is the Base of Natural Logarithms.

The **control problem** can be stated by selecting the design matrices K_p and K_v such as the position error $\tilde{\mathbf{q}}$ and the joint velocity $\dot{\tilde{\mathbf{q}}}$ vanish asymptotically, i.e., $\lim_{t \rightarrow \infty} [\tilde{\mathbf{q}}(t), \dot{\tilde{\mathbf{q}}}(t)]^T = \mathbf{0} \in \mathbb{R}^{2n}$.

Proposition. Consider the robot dynamic model (1), together with the control law (2), then the closed-loop system is globally asymptotically stable and the positioning aim $\lim_{t \rightarrow \infty} \mathbf{q}(t) = \mathbf{q}_d \wedge \lim_{t \rightarrow \infty} \dot{\mathbf{q}}(t) = \mathbf{0}$ is achieved.

Proof: The closed-loop system equation obtained by combining the robot dynamic model (1) and control scheme (2) can be written as

$$\frac{d}{dt} \begin{bmatrix} \tilde{\mathbf{q}} \\ \dot{\tilde{\mathbf{q}}} \end{bmatrix} = \begin{bmatrix} -\dot{\tilde{\mathbf{q}}} \\ M(\mathbf{q})^{-1} \left[K_p \frac{sh(\lambda \tilde{\mathbf{q}})(1 - e^{-ch(\lambda \tilde{\mathbf{q}})})}{ch(\lambda \tilde{\mathbf{q}}) + e^{-ch(\lambda \tilde{\mathbf{q}})}} - K_v \frac{sh(\lambda \dot{\tilde{\mathbf{q}}})(1 - e^{-ch(\lambda \dot{\tilde{\mathbf{q}}})})}{ch(\lambda \dot{\tilde{\mathbf{q}}}) + e^{-ch(\lambda \dot{\tilde{\mathbf{q}}})}} - C(\mathbf{q}, \dot{\tilde{\mathbf{q}}}) \dot{\tilde{\mathbf{q}}} \right] \end{bmatrix} \quad (5)$$

which is an autonomous differential equation. Now, it is demonstrated that the equilibrium point exists and it is unique. Note that $-\dot{\tilde{\mathbf{q}}} = \mathbf{0} \Rightarrow -I\dot{\tilde{\mathbf{q}}} = \mathbf{0} \Rightarrow \dot{\tilde{\mathbf{q}}} = \mathbf{0}$, where $I \in \mathbb{R}^{n \times n}$ is the identity matrix.

For the second component of the equation (5) $C(\mathbf{q}, \dot{\tilde{\mathbf{q}}}) = \mathbf{0}$ according to the property (3). $M(\mathbf{q}) > 0 \Rightarrow \exists M(\mathbf{q})^{-1} > 0$ therefore

$$\begin{aligned} M(\mathbf{q})^{-1} K_p \frac{sh(\lambda \tilde{\mathbf{q}})(1 - e^{-ch(\lambda \tilde{\mathbf{q}})})}{ch(\lambda \tilde{\mathbf{q}}) + e^{-ch(\lambda \tilde{\mathbf{q}})}} = 0 & \Leftrightarrow sh(\lambda \tilde{q}_i) = 0 \\ sh(\lambda \tilde{q}_i) = 0 & \Leftrightarrow \tilde{q}_i = 0 \end{aligned}$$

$$K_p \frac{sh(\lambda \tilde{\mathbf{q}})(1 - e^{-ch(\lambda \tilde{\mathbf{q}})})}{ch(\lambda \tilde{\mathbf{q}}) + e^{-ch(\lambda \tilde{\mathbf{q}})}} = 0 \Leftrightarrow \tilde{q}_i = 0$$

with $k_{p_i} \in \mathbb{R}_+$, $K_p = diagonal(k_{p_i})$.

Therefore, the origin of the state space is its unique equilibrium point.

To carry out the stability analysis of equation (5), the following Lyapunov function candidate is proposed:

$$\begin{aligned} V(\tilde{\mathbf{q}}, \dot{\tilde{\mathbf{q}}}) = & \frac{1}{2} \dot{\tilde{\mathbf{q}}}^T M(\mathbf{q}) \dot{\tilde{\mathbf{q}}} \\ & + \begin{bmatrix} \sqrt{\ln\left(\frac{ch(\lambda \tilde{q}_1) + e^{-ch(\lambda \tilde{q}_1)}}{1 + e^{-1}}\right)} \\ \vdots \\ \sqrt{\ln\left(\frac{ch(\lambda \tilde{q}_n) + e^{-ch(\lambda \tilde{q}_n)}}{1 + e^{-1}}\right)} \end{bmatrix}^T \\ & \Lambda K_p \begin{bmatrix} \sqrt{\ln\left(\frac{ch(\lambda \tilde{q}_1) + e^{-ch(\lambda \tilde{q}_1)}}{1 + e^{-1}}\right)} \\ \vdots \\ \sqrt{\ln\left(\frac{ch(\lambda \tilde{q}_n) + e^{-ch(\lambda \tilde{q}_n)}}{1 + e^{-1}}\right)} \end{bmatrix} \end{aligned} \quad (6)$$

where Λ is a diagonal matrix and it is represented as:

$$\Lambda = \begin{bmatrix} \frac{1}{\lambda_1} & \cdots & 0 \\ \vdots & \ddots & \vdots \\ 0 & \cdots & \frac{1}{\lambda_n} \end{bmatrix}$$

The first term of $V(\tilde{\mathbf{q}}, \dot{\mathbf{q}})$ is a positive definite function with respect to $\dot{\mathbf{q}}$ because $M(\mathbf{q})$ is a positive definite matrix. The second term of Lyapunov function candidate (6), which can be interpreted as a potential energy induced by the position error is also a positive definite function with respect to position error $\tilde{\mathbf{q}}$, because K_p is a positive definite diagonal matrix.

Therefore, the Lyapunov function candidate (6) is a radially unbounded and a globally positive definite function. The time derivative of Lyapunov function candidate (6) is:

$$\begin{aligned} \dot{V}(\tilde{\mathbf{q}}, \dot{\mathbf{q}}) &= \dot{\mathbf{q}}^T M(\mathbf{q})\ddot{\mathbf{q}} + \frac{1}{2}\dot{\mathbf{q}}^T \dot{M}(\mathbf{q})\dot{\mathbf{q}} \\ &+ \left[\begin{array}{c} \sqrt{\ln\left(\frac{ch(\lambda\tilde{q}_1)+e^{-ch(\lambda\tilde{q}_1)}}{1+e^{-1}}\right)} \\ \vdots \\ \sqrt{\ln\left(\frac{ch(\lambda\tilde{q}_n)+e^{-ch(\lambda\tilde{q}_n)}}{1+e^{-1}}\right)} \end{array} \right]^T \\ &K_p \left[\begin{array}{c} \frac{sh(\lambda\tilde{q}_1)(1-e^{-ch(\lambda\tilde{q}_1)})}{ch(\lambda\tilde{q}_1)+e^{-ch(\lambda\tilde{q}_1)}} \\ \vdots \\ \frac{sh(\lambda\tilde{q}_n)(1-e^{-ch(\lambda\tilde{q}_n)})}{ch(\lambda\tilde{q}_n)+e^{-ch(\lambda\tilde{q}_n)}} \end{array} \right] \dot{\tilde{\mathbf{q}}} \end{aligned} \quad (7)$$

after simplifying some terms:

$$\begin{aligned} \dot{V}(\tilde{\mathbf{q}}, \dot{\mathbf{q}}) &= \dot{\mathbf{q}}^T M(\mathbf{q})\ddot{\mathbf{q}} + \frac{1}{2}\dot{\mathbf{q}}^T \dot{M}(\mathbf{q})\dot{\mathbf{q}} \\ &- \dot{\mathbf{q}}^T K_p \frac{sh(\lambda\tilde{q}_i)(1-e^{-ch(\lambda\tilde{q}_i)})}{ch(\lambda\tilde{q}_i)+e^{-ch(\lambda\tilde{q}_i)}} \end{aligned} \quad (8)$$

along the trajectories of the closed-loop equation (5) is:

$$\begin{aligned} \dot{V}(\tilde{\mathbf{q}}, \dot{\mathbf{q}}) &= \dot{\mathbf{q}}^T M(\mathbf{q}) \left[M(\mathbf{q})^{-1} \left[K_p \frac{sh(\lambda\tilde{\mathbf{q}})(1-e^{-ch(\lambda\tilde{\mathbf{q}})})}{ch(\lambda\tilde{\mathbf{q}})+e^{-ch(\lambda\tilde{\mathbf{q}})}} \right. \right. \\ &- K_v \frac{sh(\lambda\dot{\mathbf{q}})(1-e^{-ch(\lambda\dot{\mathbf{q}})})}{ch(\lambda\dot{\mathbf{q}})+e^{-ch(\lambda\dot{\mathbf{q}})}} - C(\mathbf{q}, \dot{\mathbf{q}})\dot{\mathbf{q}} \left. \left. \right] \right] \\ &+ \frac{1}{2}\dot{\mathbf{q}}^T \dot{M}(\mathbf{q})\dot{\mathbf{q}} - \dot{\mathbf{q}}^T K_p \frac{sh(\lambda\tilde{q}_i)(1-e^{-ch(\lambda\tilde{q}_i)})}{ch(\lambda\tilde{q}_i)+e^{-ch(\lambda\tilde{q}_i)}} \end{aligned} \quad (9)$$

and after some algebra is:

$$\begin{aligned} \dot{V}(\tilde{\mathbf{q}}, \dot{\mathbf{q}}) &= \dot{\mathbf{q}}^T K_p \frac{sh(\lambda\tilde{q}_i)(1-e^{-ch(\lambda\tilde{q}_i)})}{ch(\lambda\tilde{q}_i)+e^{-ch(\lambda\tilde{q}_i)}} \\ &- \dot{\mathbf{q}}^T K_v \frac{sh(\lambda\dot{q}_i)(1-e^{-ch(\lambda\dot{q}_i)})}{ch(\lambda\dot{q}_i)+e^{-ch(\lambda\dot{q}_i)}} \\ &- \dot{\mathbf{q}}^T C(\mathbf{q}, \dot{\mathbf{q}})\dot{\mathbf{q}} + \frac{1}{2}\dot{\mathbf{q}}^T \dot{M}(\mathbf{q})\dot{\mathbf{q}} \\ &- \dot{\mathbf{q}}^T K_p \frac{sh(\lambda\tilde{q}_i)(1-e^{-ch(\lambda\tilde{q}_i)})}{ch(\lambda\tilde{q}_i)+e^{-ch(\lambda\tilde{q}_i)}} \end{aligned} \quad (10)$$

then:

$$\begin{aligned} \dot{V}(\tilde{\mathbf{q}}, \dot{\mathbf{q}}) &= -\dot{\mathbf{q}}^T K_v \frac{sh(\lambda\dot{q}_i)(1-e^{-ch(\lambda\dot{q}_i)})}{ch(\lambda\dot{q}_i)+e^{-ch(\lambda\dot{q}_i)}} \\ &+ \dot{\mathbf{q}}^T \left[\frac{1}{2}\dot{M}(\mathbf{q}) - C(\mathbf{q}, \dot{\mathbf{q}}) \right] \dot{\mathbf{q}} \end{aligned} \quad (11)$$

and using property 2 it can be written as:

$$\dot{V}(\tilde{\mathbf{q}}, \dot{\mathbf{q}}) = -\dot{\mathbf{q}} K_v \begin{bmatrix} \frac{sh(\lambda\dot{q}_1)(1-e^{-ch(\lambda\dot{q}_1)})}{ch(\lambda\dot{q}_1)+e^{-ch(\lambda\dot{q}_1)}} \\ \vdots \\ \frac{sh(\lambda\dot{q}_n)(1-e^{-ch(\lambda\dot{q}_n)})}{ch(\lambda\dot{q}_n)+e^{-ch(\lambda\dot{q}_n)}} \end{bmatrix} \leq 0 \quad (12)$$

which is a negative semidefinite function. We therefore concluded that the equilibrium point is stable. In order to prove the asymptotic stability in a global way, we make use of the autonomous nature of closed-loop (2) when we applied *LaSalle's invariance principle*:

In the region

$$\Omega = \left\{ \begin{bmatrix} \tilde{\mathbf{q}} \\ \dot{\mathbf{q}} \end{bmatrix} \in \mathbb{R}^n : \dot{V}(\tilde{\mathbf{q}}, \dot{\mathbf{q}}) = 0 \right\} \quad (13)$$

the unique invariant is $[\tilde{\mathbf{q}}^T \dot{\mathbf{q}}^T]^T = 0 \in \mathbb{R}^{2n}$, therefore

$$\lim_{t \rightarrow \infty} \begin{bmatrix} \tilde{\mathbf{q}}(t) \\ \dot{\mathbf{q}}(t) \end{bmatrix} \rightarrow 0.$$

IV. EXPERIMENTAL SET-UP

An experimental system for researching robot control algorithms has been designed and built at The "Benemérita Universidad Autónoma de Puebla". It is a direct-drive robot manipulator with three degrees of freedom moving in 3-dimensional space (see Fig. 1).



Fig. 1. Experimental robot. Home position

The experimental robot consists of links made of 6061 aluminum, actuated by brushless direct drive servo actuator

from Parker Compumotor to drive the joints without gear reduction. Advantages of this type of direct-drive actuator include freedom from backlash and significantly lower joint friction compared with actuators composed by gear drives. The motors used in the experimental robot are listed in Table I.

TABLE I
SERVO ACTUATORS OF THE EXPERIMENTAL ROBOT.

Link	Model	Torque [Nm]	p/rev
Base	DM-1015B-60	15	2621440
Shoulder	DM-1050A-115	50	4096000
Elbow	DM-1004C-115	4	2621440

The servos are operated in torque mode, so the motors act as torque source and they accept an analog voltage as a reference of torque signal. Position information is obtained from incremental encoders located on the motors. The standard backwards difference algorithm applied to the joint position measurements are used to generate the velocity signals. The manipulator workspace is a sphere with a radius of 1m.

Besides position sensors and motor drivers, the manipulator also includes a motion control board manufactured by Precision MicroDynamic Inc., which is used to obtain the joint positions. The control algorithm runs on a Pentium-II (333 Mhz) host computer.

With reference to our direct-drive robot, only the gravitational vector is required to implement the new family of controllers (2), which is available in [20]

$$\mathbf{g}(\mathbf{q}) = \begin{bmatrix} 0 \\ 1,02 \sin(q_1) + 0,20 \sin(q_1 + q_2) \\ 0,20 \sin(q_1 + q_2) \end{bmatrix} \quad [\text{Nm}].$$

V. EXPERIMENTAL RESULTS

In this Section an experimental comparison of four position controllers on a three-degrees-of-freedom direct-drive robot manipulator which support our theoretical developments is presented. To investigate the performance among controllers, they have been classified as HE1, HE2 and HE3 for the hyperbolic and exponent family where the coefficient $\lambda = 1, 2, \text{ and } 3$, respectively. We denote the PD for the simple PD controller.

In order to compare the performance of the controllers on direct - drive robot, an experiment of position control whose objective is to move the manipulator end - effector from its initial position to a fixed desired target has been designed. For the present application there are two configurations of desired joint positions, the first one as: $[q_{d1}, q_{d2}, q_{d3}]^T = [45, 45, 90]^T$ degrees and the second one as $[q_{d1}, q_{d2}, q_{d3}]^T = [135, 70, 110]^T$ degrees, where q_{d1}, q_{d2}, q_{d3} represents the base, shoulder, and elbow joints, respectively. The initial positions and velocities were set to zero (for example in home position). The friction phenomena was not modeled for compensation purpose. As a result, all the controllers did not show any type of friction compensation, therefore it has been decided to consider the friction unmodeled dynamics. Evaluated controllers have been written in C language. The sampling rate was executed at 2.5

msec. Fig. 1 and Fig. 2 show the initial and one of the desired configurations for the experimental robot, respectively.

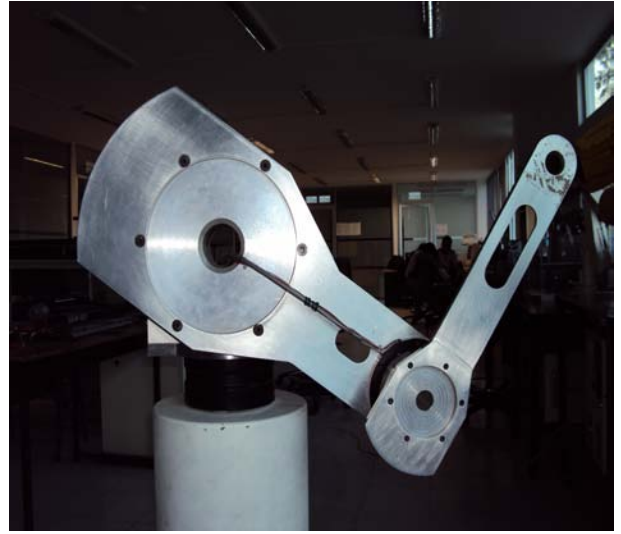


Fig. 2. Desired position for experimental robot

VI. EXPERIMENTAL RESULTS FOR THE HYPERBOLIC EXPONENTIAL FAMILY CONTROLLER

From equation (2), with $n = 3$ degrees of freedom for the experimental arm, (see Fig.1) the following class of controllers can be obtained:

With the coefficient $\lambda = 1$, this member of the family is called HE1, the equation for the three joints of the robot arm are as follows:

$$\begin{aligned} \tau_{HE1_1} &= K_{p1} \frac{sh(\tilde{q}_1)(1 - e^{-ch(\tilde{q}_1)})}{ch(\tilde{q}_1) + e^{-ch(\tilde{q}_1)}} \\ &\quad - K_{v1} \frac{sh(\alpha_{11}\dot{q}_1)(1 - e^{-ch(\alpha_{11}\dot{q}_1)})}{ch(\alpha_{11}\dot{q}_1) + e^{-ch(\alpha_{11}\dot{q}_1)}} \\ \tau_{HE1_2} &= K_{p1} \frac{sh(\tilde{q}_2)(1 - e^{-ch(\tilde{q}_2)})}{ch(\tilde{q}_2) + e^{-ch(\tilde{q}_2)}} \\ &\quad - K_{v1} \frac{sh(\alpha_{12}\dot{q}_2)(1 - e^{-ch(\alpha_{12}\dot{q}_2)})}{ch(\alpha_{12}\dot{q}_2) + e^{-ch(\alpha_{12}\dot{q}_2)}} \\ &\quad + 1,02 \sin(q_2) + 0,2 \sin(q_2 + q_3) \\ \tau_{HE1_3} &= K_{p1} \frac{sh(\tilde{q}_3)(1 - e^{-ch(\tilde{q}_3)})}{ch(\tilde{q}_3) + e^{-ch(\tilde{q}_3)}} \\ &\quad - K_{v1} \frac{sh(\alpha_{13}\dot{q}_3)(1 - e^{-ch(\alpha_{13}\dot{q}_3)})}{ch(\alpha_{13}\dot{q}_3) + e^{-ch(\alpha_{13}\dot{q}_3)}} \\ &\quad + 0,2 \sin(q_2 + q_3) \end{aligned} \quad (14)$$

With the coefficient $\lambda = 2$, this member of the family is called HE2, the equation for the three joints of the robot arm are as follows:

$$\begin{aligned} \tau_{HE2_1} &= K_{p1} \frac{sh(2 * \tilde{q}_1)(1 - e^{-ch(2*\tilde{q}_1)})}{ch(2 * \tilde{q}_1) + e^{-ch(2*\tilde{q}_1)}} \\ &\quad - K_{v1} \frac{sh(\alpha_{21}\dot{q}_1)(1 - e^{-ch(\alpha_{21}\dot{q}_1)})}{ch(\alpha_{21}\dot{q}_1) + e^{-ch(\alpha_{21}\dot{q}_1)}} \\ \tau_{HE2_2} &= K_{p1} \frac{sh(2 * \tilde{q}_2)(1 - e^{-ch(2*\tilde{q}_2)})}{ch(2 * \tilde{q}_2) + e^{-ch(2*\tilde{q}_2)}} \end{aligned}$$

$$\begin{aligned} \tau_{HE2_3} = & -K_{v1} \frac{sh(\alpha_{22}\dot{q}_2)(1 - e^{-ch(\alpha_{22}\dot{q}_2)})}{ch(\alpha_{22}\dot{q}_2) + e^{-ch(\alpha_{22}\dot{q}_2)}} \\ & + 1,02 \sin(q_2) + 0,2 \sin(q_2 + q_3) \\ & -K_{p1} \frac{sh(2 * \tilde{q}_3)(1 - e^{-ch(2*\tilde{q}_3)})}{ch(2 * \tilde{q}_3) + e^{-ch(2*\tilde{q}_3)}} \\ & -K_{v1} \frac{sh(\alpha_{23}\dot{q}_3)(1 - e^{-ch(\alpha_{23}\dot{q}_3)})}{ch(\alpha_{23}\dot{q}_3) + e^{-ch(\alpha_{23}\dot{q}_3)}} \\ & + 0,2 \sin(q_2 + q_3) \end{aligned} \quad (15)$$

With the coefficient $\lambda = 3$, this member of the family is called HE3, the equation for the three joints of the robot arm are as follows:

$$\begin{aligned} \tau_{HE3_1} = & K_{p1} \frac{sh(3 * \tilde{q}_1)(1 - e^{-ch(3*\tilde{q}_1)})}{ch(3 * \tilde{q}_1) + e^{-ch(3*\tilde{q}_1)}} \\ & -K_{v1} \frac{sh(\alpha_{31}\dot{q}_1)(1 - e^{-ch(\alpha_{31}\dot{q}_1)})}{ch(\alpha_{31}\dot{q}_1) + e^{-ch(\alpha_{31}\dot{q}_1)}} \\ \tau_{HE3_2} = & K_{p1} \frac{sh(3 * \tilde{q}_2)(1 - e^{-ch(3*\tilde{q}_2)})}{ch(3 * \tilde{q}_2) + e^{-ch(3*\tilde{q}_2)}} \\ & -K_{v1} \frac{sh(\alpha_{32}\dot{q}_2)(1 - e^{-ch(\alpha_{32}\dot{q}_2)})}{ch(\alpha_{32}\dot{q}_2) + e^{-ch(\alpha_{32}\dot{q}_2)}} \\ & + 1,02 \sin(q_2) + 0,2 \sin(q_2 + q_3) \\ \tau_{HE3_3} = & K_{p1} \frac{sh(3 * \tilde{q}_3)(1 - e^{-ch(3*\tilde{q}_3)})}{ch(3 * \tilde{q}_3) + e^{-ch(3*\tilde{q}_3)}} \\ & -K_{v1} \frac{sh(\alpha_{33}\dot{q}_3)(1 - e^{-ch(\alpha_{33}\dot{q}_3)})}{ch(\alpha_{33}\dot{q}_3) + e^{-ch(\alpha_{33}\dot{q}_3)}} \\ & + 0,2 \sin(q_2 + q_3) \end{aligned} \quad (16)$$

where $(\tau_{HE1_1}, \tau_{HE2_1}, \tau_{HE3_1}), (\tau_{HE1_2}, \tau_{HE2_2}, \tau_{HE3_2})$ and $(\tau_{HE1_3}, \tau_{HE2_3}, \tau_{HE3_3})$ represent the applied torques for the base, shoulder, and elbow joints, respectively. The controllers gains were selected empirically. However, several trials for selecting gains were necessary in order to ensure an acceptable behavior in practice, that is, fast response and a smaller steady - state error.

In order to avoid torque saturation of the actuators, but to function in its linear part, the proportional gains were chosen such that $\tau < \|\tau_{max}\|$, where τ_{max} represents the maximum applied torque of the i th joint (see limits of actuators in Table I).

The empirical formula that was used to select the tuning of the proportional gain is given by: $k_{pi} = 80\% \tau_{imax} / q_{di}$. For that reason the values for k_{p1}, k_{p2} and k_{p3} are: 12, 32 and 3.2 respectively, that correspond to the 80% of the nominal torque of the actuators, see Table II.

TABLE II
SETTINGS FOR EXPONENT HYPERBOLIC, k_{pi} VALUES.

k_p	[Nm]
k_{p1}	12
k_{p2}	32
k_{p3}	3.2

With the proportional gains fixed, derivative ones were adjusted to obtain a low under - damped response. For a lower α a proportional relation between velocity and derivative value is obtained.

For each member of this proposed family of controllers: HE1, HE2, HE3 that correspond to the coefficient, $\lambda = 1, 2$, and 3, there are particularly K_p and K_v matrices.

VI-A. Desired position $[45, 45, 90]^T$

For the first configuration of desired positions, that is $[q_{d1}, q_{d2}, q_{d3}]^T = [45, 45, 90]^T$ degrees, values for k_{vij} and α_{ij} are shown in Table III.

TABLE III
SETTINGS FOR EXPONENT HYPERBOLIC, λ_i, k_{vij} AND α_{ij} VALUES
 $[q_{d1}, q_{d2}, q_{d3}]^T = [45, 45, 90]^T$ DEGREES

	k_v	[Nm]	α	$[\frac{rad*s}{degrees}]$
$\lambda = 1$	k_{v1}	3	α_{11}	0.015
	k_{v2}	0.5	α_{12}	0.002
	k_{v3}	0.1	α_{13}	0.0002
$\lambda = 2$	k_{v1}	17	α_{21}	0.01
	k_{v1}	1.4	α_{22}	0.001
	k_{v1}	0.04	α_{23}	0.001
$\lambda = 3$	k_{v1}	28	α_{31}	0.01
	k_{v1}	0.32	α_{32}	0.006
	k_{v1}	2.4	α_{33}	0.004

Fig. 3 to 8 contain the experimental results of the hyperbolic and exponential family. There are three members of the family HE1, HE2, HE3, the graphic of position error and applied torque are shown for each one. The graphics of position error show that the three links tend to a small neighborhood near zero. This characteristic demonstrates the properties of the proposed family. The graphic of applied torque shows that the actuator works in its linear zone but not in that of saturation.

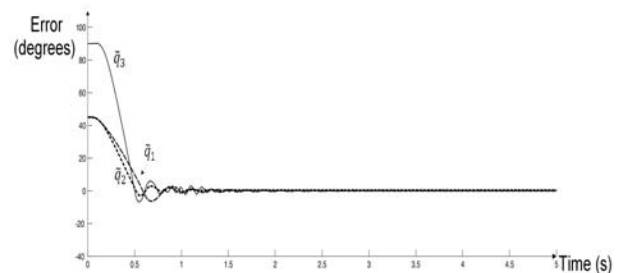


Fig. 3. Position errors of the HE1 controller.

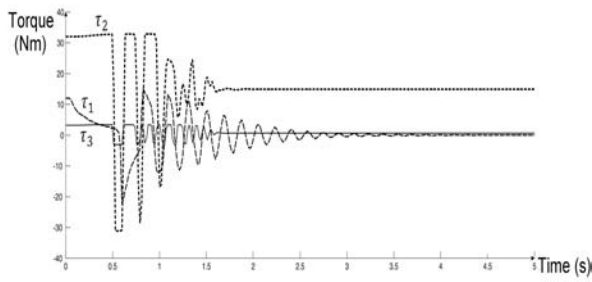


Fig. 4. Applied torques of the HE1 controller.

Fig. 3 and 4, correspond to the HE1 controller. The steady state position begins approximately at $t = 2$ sec, and $[\tilde{q}_1, \tilde{q}_2, \tilde{q}_3]^T = [0,001, 0,399, 0,113]^T$ degrees.

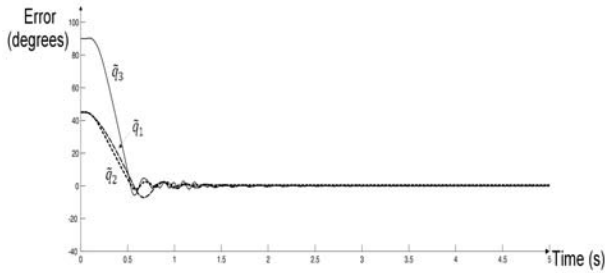


Fig. 5. Position errors of the HE2 controller.

Fig. 5 and 6, correspond to the HE2 controller. The steady state position begins approximately at $t = 1.5$ sec., and $[\tilde{q}_1, \tilde{q}_2, \tilde{q}_3]^T = [0,001, 0,385, 0,096]^T$ degrees.

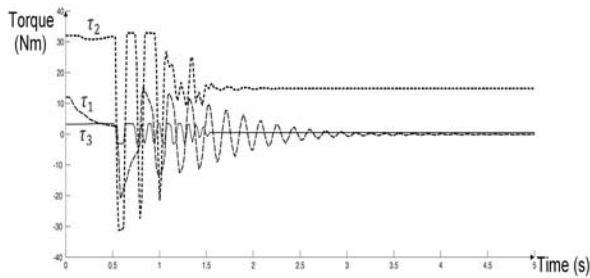


Fig. 6. Applied torques of the HE2 controller.

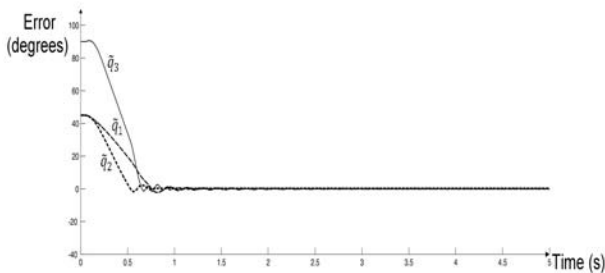


Fig. 7. Position errors of the HE3 controller.

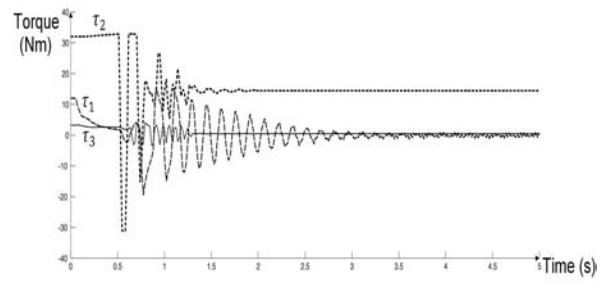


Fig. 8. Applied torques of the HE3 controller.

Fig. 7 and 8, correspond to the HE3 controller. The steady state position begins at $t = 3$ sec., and $[\tilde{q}_1, \tilde{q}_2, \tilde{q}_3]^T = [0,009, 0,298, 0,076]^T$ degrees.

VI-B. Desired position $[135, 70, 110]^T$

For the second configuration of desired positions, that is $[q_{d1}, q_{d2}, q_{d3}]^T = [135, 70, 110]^T$ degrees, values for k_{vij} and α_{ij} are shown in Table IV.

TABLE IV
SETTINGS FOR EXPONENT HYPERBOLIC, λ_i , k_{vij} AND α_{ij} VALUES FOR $[q_{d1}, q_{d2}, q_{d3}]^T = [135, 70, 110]^T$ DEGREES

	k_v	[Nm]	α	$[\frac{rads}{degrees}]$
$\lambda = 1$	k_{v1}	9	α_{11}	0.01
	k_{v2}	0.1	α_{12}	0.01
	k_{v3}	0.1	α_{13}	0.0002
$\lambda = 2$	k_{v1}	50	α_{21}	0.02
	k_{v1}	0.001	α_{22}	0.040
	k_{v1}	0.15	α_{23}	0.002
$\lambda = 3$	k_{v1}	22	α_{31}	0.013
	k_{v1}	0.05	α_{32}	0.01
	k_{v1}	1	α_{33}	0.04

Fig. 9 to 14 contain the experimental results of the hyperbolic and exponential family for the desired position $[q_{d1}, q_{d2}, q_{d3}]^T = [135, 70, 110]^T$ degrees.

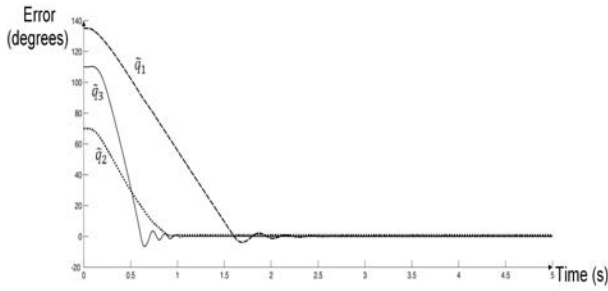


Fig. 9. Position errors of the HE1 controller.

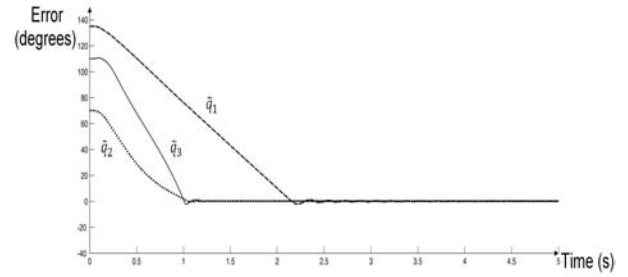


Fig. 13. Position errors of the HE3 controller.

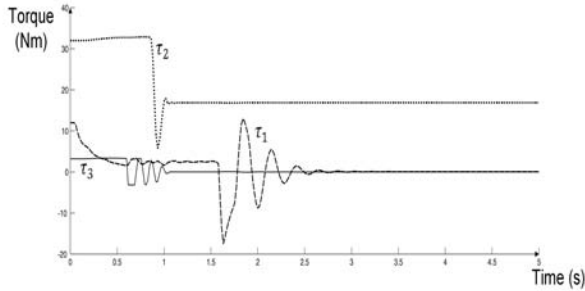


Fig. 10. Applied torques of the HE1 controller.

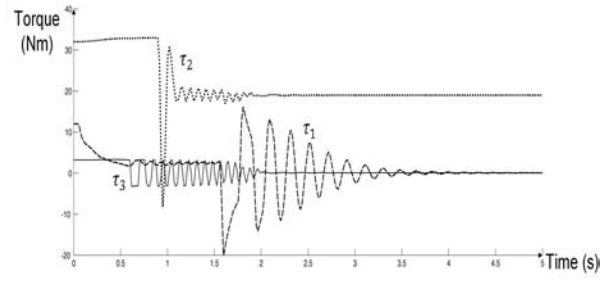


Fig. 14. Applied torques of the HE3 controller.

Fig. 9 and 10, correspond to the HE1 controller. The steady state position begins approximately at $t = 2$ sec, and $[\tilde{q}_1, \tilde{q}_2, \tilde{q}_3]^T = [0,011, 0,95, -0,0028]^T$ degrees.

Fig. 13 and 14, correspond to the HE3 controller. The steady state position begins at $t = 3$ sec., and $[\tilde{q}_1, \tilde{q}_2, \tilde{q}_3]^T = [-0,030, 0,31, 0,0005]^T$ degrees.

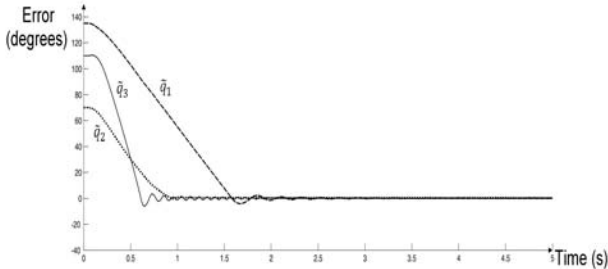


Fig. 11. Position errors of the HE2 controller.

Fig. 11 and 12, correspond to the HE2 controller. The steady state position begins approximately at $t = 2.5$ sec., and $[\tilde{q}_1, \tilde{q}_2, \tilde{q}_3]^T = [0,004, 0,53, 0,027]^T$ degrees.

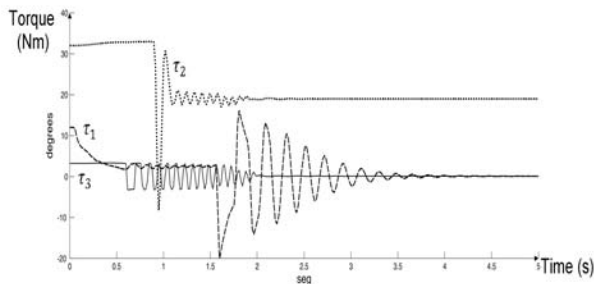


Fig. 12. Applied torques of the HE2 controller.

VII. EXPERIMENTAL RESULTS FOR THE PD CONTROLLER

This Section presents the results of the PD controller. The desired positions and the initial conditions were the same as in the previous Section. Fig. 15 to 18 contain the experimental results of this part. The PD controller for the three degrees of freedom robot arm are given by the following equations.

$$\begin{aligned} \tau_{PD1} &= K_{p1}(\tilde{q}_1) - K_{v1}(\dot{q}_1) \\ \tau_{PD2} &= K_{p2}(\tilde{q}_2) - K_{v2}(\dot{q}_2) \\ &\quad + 1,02 \sin(q_2) + 0,2 \sin(q_2 + q_3) \\ \tau_{PD3} &= K_{p3}(\tilde{q}_3) - K_{v3}(\dot{q}_3) \\ &\quad + 0,2 \sin(q_2 + q_3) \end{aligned} \quad (17)$$

where τ_{PD1} , τ_{PD2} and τ_{PD3} represent the applied torques for the base, shoulder, and elbow joints, respectively.

Extensive experiments were carried out with the PD controllers to select their gains, such that the best time response without overshoot and minimum steady - state position error were obtained without entering the saturation zone of the actuator's torques. The PD gains were selected as: $k_{pi} = 80\% | \tau_{i_{max}} | / \tilde{q}_i(0)$ and $k_{vi} \ll k_{pi}$. After a trial and error procedure, proportional and derivative gains have been selected as suitable choices for preventing the actuators from saturation. Fig. 16 and 18 are inside the limits of torque for its respective actuator but not in the saturation zone.

Values for k_{pi} and k_{vi} for the PD controller are shown in Table V.

TABLE V
SETTINGS FOR THE PD CONTROLLER.

$[q_{d1}, q_{d2}, q_{d3}]^T$	k_p	[Nm]	k_v	$[\frac{rad*s}{degrees}]$
$[45, 45, 90]^T$ [degrees]	k_{p1}	0.3	k_{v1}	6E-4
	k_{p2}	0.9	k_{v2}	0.01
	k_{p3}	0.045	k_{v3}	0.001
$[135, 70, 110]^T$ [degrees]	k_{p1}	0.09	k_{v1}	4.0
	k_{p2}	0.46	k_{v2}	10
	k_{p3}	0.03	k_{v3}	0.2

VII-A. Desired position $[45, 45, 90]^T$

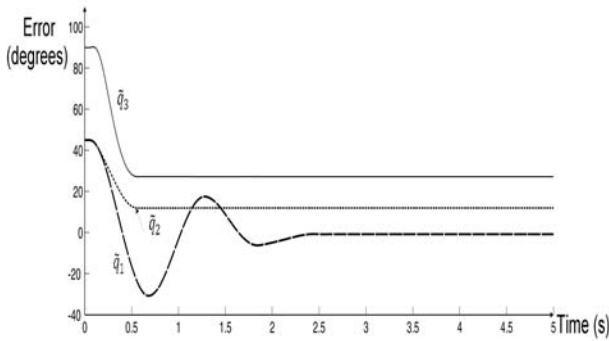


Fig. 15. Position errors of the PD controller.

Fig. 15 contains the experimental result of position errors of the PD controller. The steady state position begins approximately at $t = 2.5$ sec., and $[\tilde{q}_1, \tilde{q}_2, \tilde{q}_3]^T = [0, 8108, 11, 9658, 27, 1879]^T$ degrees. Fig. 16 show the applied torque with the PD controller for the base, shoulder and elbow.

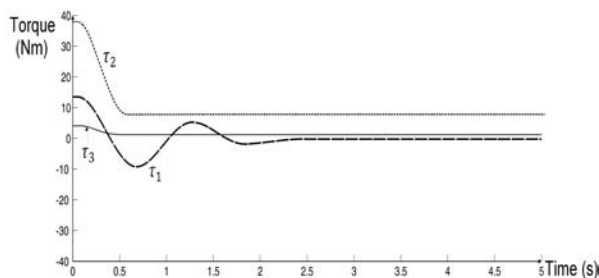


Fig. 16. Applied torques of the PD controller.

VII-B. Desired position $[135, 70, 110]^T$

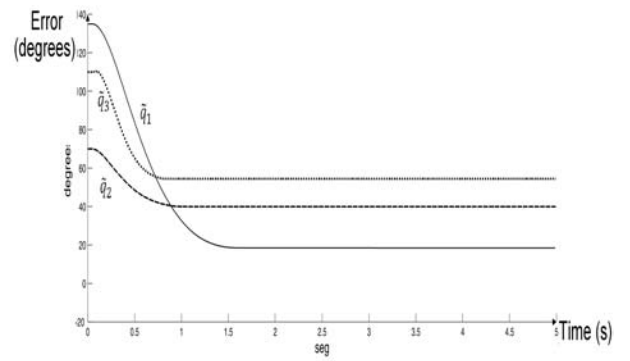


Fig. 17. Position errors of the PD controller.

Fig. 17 contains the experimental result of position errors of the PD controller. The steady state position begins approximately at $t = 1.5$ sec., and $[\tilde{q}_1, \tilde{q}_2, \tilde{q}_3]^T = [18, 39, 54]^T$ degrees.

Fig. 18 shows the applied torque with the PD controller for the base, shoulder and elbow.

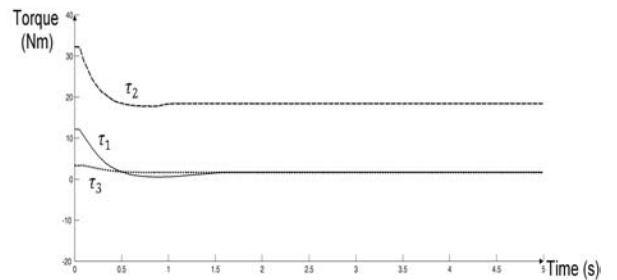


Fig. 18. Applied torques of the PD controller.

VIII. INDICES OF PERFORMANCE

The robot manipulators are very complex mechanical systems, due to the nonlinear and multivariable nature of their dynamical behavior. For this reason, in the robotic community there are no well-established criteria for a proper evaluation of controllers for robots. However, it is accepted in practice to compare the performance of controllers by using the scalar-valued \mathcal{L}^2 norm as an objective numerical measure for an entire error curve Whitcomb et. al [21] De Jager & Banens [22] Berghuis et. al [23] Jaritz & Spong [24]. The $\mathcal{L}^2[\tilde{q}]$ norm measures the root-mean-square average of the \tilde{q} position error, which is given by:

$$\mathcal{L}^2[\tilde{q}] = \sqrt{\frac{1}{t-t_0} \int_{t_0}^t \|\tilde{q}\|^2 dt} \quad (18)$$

where $t_0, t \in \mathbb{R}_+$ are the initial and final times, respectively. A smaller $\mathcal{L}^2[\tilde{q}]$ represents smaller position error and it gives the best performance of the evaluated controller. The data are compared with respect to the PD controller. To average out stochastic influences, the data represent the mean of root -

mean - square position error vector norm of ten runs.

Fig. 19 and 20 show the performance indices of all the controllers, for $[q_{d1}, q_{d2}, q_{d3}]^T = [45, 45, 90]^T$ degrees and $[q_{d1}, q_{d2}, q_{d3}]^T = [135, 70, 110]^T$ degrees respectively. The overall results are summarized by Table VI which includes the performance indices of all the controllers. In general the proposed controller improves the performance of the PD, the two first members of the proposed family (HE1, HE2) in about 32 % - 33 % and the last member (HE3) in about 21 % - 24 %.

The result from one run to another was observed, and the difference with the average are the following: 0.5 %, 0.6 %, 1.6 %, 0.7 % for HE1, HE2, HE3, and the PD respectively, which underline the repeatability of the experiments.

TABLE VI
 \mathcal{L}^2 NORM FOR TRANSIENT AND STATIONARY STATES.

$[q_{d1}, q_{d2}, q_{d3}]^T$		\mathcal{L}^2 [degrees]	difference [%]
$[45, 45, 90]^T$	HE1	25.67	32
	HE2	25.64	32
	HE3	27.79	21
	PD	37.7	-
$[135, 70, 110]^T$	HE1	57.8	33
	HE2	57.7	33
	HE3	65.4	24
	PD	85.7	-

In order to compare the error, the values of \mathcal{L}^2 norm for the stationary state have been obtained (Fig. 21 and Fig. 22) These values are taken in the last second of each test, between the 4th and 5th second, and are summarized in table VII.

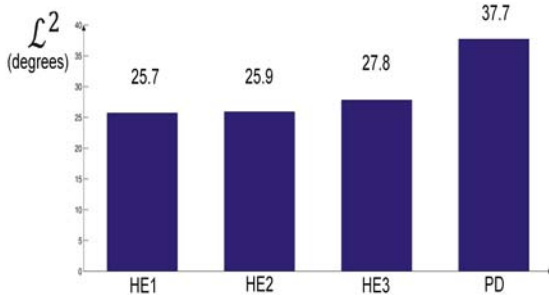


Fig. 19. Performance index for transient and stationary states.

TABLE VII
 \mathcal{L}^2 NORM FOR STATIONARY STATE.

$[q_{d1}, q_{d2}, q_{d3}]^T$		\mathcal{L}^2 [degrees]	difference [%]
$[45, 45, 90]^T$	HE1	0.15	99
	HE2	0.14	99
	HE3	0.10	99
	PD	9.7	-
$[135, 70, 110]^T$	HE1	0.43	95
	HE2	0.24	97
	HE3	0.14	98
	PD	8.35	-

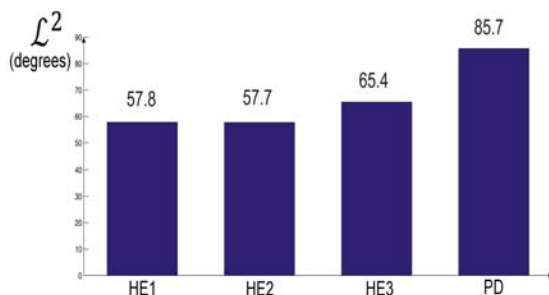


Fig. 20. Performance index for transient and stationary states

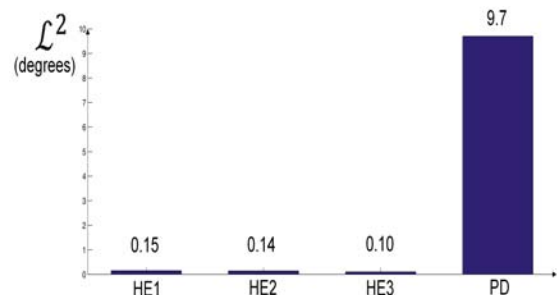


Fig. 21. Performance index for stationary state case.

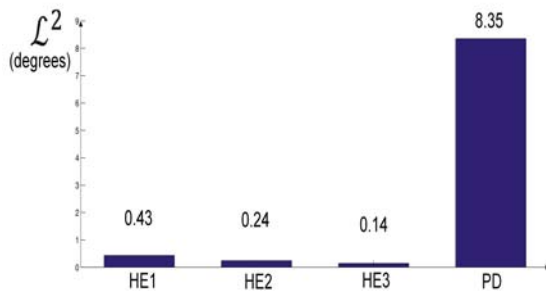


Fig. 22. Performance index for stationary state case.

Fig. 21 and 22 shows the results and evidence for the poor performance of the PD controller in the stationary state.

The \mathcal{L}^2 norm for the stationary state of the proposed controller is about 95 % - 99 % less than the PD controller.

IX. CONCLUSIONS

The hyperbolic and exponential family of controllers for position control of robot manipulators has been introduced in this paper. A rigorous stability analysis has been carried out and the theoretical results determinate conditions for ensuring global regulation.

The performance of the new scheme was compared with a well known algorithm such as the PD controller by using a real - time experimental comparison on a three degrees of freedom direct - drive robot. From the experimental results the new scheme was sufficient to produce a brief transient and minimum steady - state position error in comparison with the PD controllers that showed to be less robust than the proposed scheme.

This new family show the less $\mathcal{L}^2[\tilde{q}]$ norm, therefore the best performance than the evaluated controller and the less $\mathcal{L}^2[\tilde{q}]$ norm for stationary state, which indicate a smaller error than with the PD controller. For this reason, the usefulness of the proposed family can be concluded to represent an attractive scheme from a practical viewpoint; for example in manufacturing systems.

REFERENCES

- [1] V. Santibañez, R. Kelly, and M. Llama. A novel global asymptotic stable set-point fuzzy controller with bounded torques for robot manipulators. *IEEE Transactions on Fuzzy Systems*. Vol. 13, No.3, 2005, pp.362-372.
- [2] R. Kelly, A tuning procedure for stable PID control of robot manipulators. *Robotica, Cambridge University Press*, Vol. 13, 1995, pp.141-148.
- [3] L. Sciavicco, & B. Siciliano, *Modeling and Control of Robot Manipulators* The McGraw-Hill Companies, Inc. 1996.
- [4] C. Canudas, B. Siciliano, & G. Bastin, *Theory of Robot Control*. Springer, 1996.
- [5] H. K. Khalil, *Nonlinear Systems*. Prentice-Hall, 2002.
- [6] M. Takegaki, & S. Arimoto, A new feedback method for dynamic control of manipulators. *J. Dyn. Syst. Meas. Control Transactions. ASME* Vol. 103, 1981, pp.119-125.
- [7] S. Arimoto, and F. Miyazaki, *Stability and robustness of PD feedback control with gravity compensation for robot manipulator*. Robotics: Theory and Application - DSC, F. W. Paul and D. Youcef-Toumi Eds. Vol.3, 1986, pp. 67-72.
- [8] M. Ho & Y. Tu, Position control of a single - link flexible manipulator using H_∞-based PID control. *IEEE Transactions Control Theory and Applications*. Vol. 153, No.5, 2006, pp.615 -622.
- [9] H. Arai & S. Tachi, Position control of manipulator with passive joints using dynamic coupling. *IEEE Transactions on Robotic and Automation*. Vol. 7, No. 4, 2002, pp.528 - 534.
- [10] W. Wang, S. Lu & C. Hsu, Experiments on the position control of a one - link flexible robot arm. *IEEE Transactions on Robotics and Automation*. Vol.5, No.3, 2002, pp.373 - 377.
- [11] R. Kelly, & R. Carelli, A class of nonlinear PD-Type controllers for robot manipulators. *Journal of Robotic Systems*. Vol.13, No.12, 1996, pp.793-802.
- [12] H. Seraji A new class of nonlinear PID controllers with robotic applications. *Journal of Robotic Systems*. Vol. 15, No.3, 1998, pp.61-81.
- [13] T. C. Hsia, Robustness analysis of a PD controller with approximate gravity compensation for robot manipulator control. *Journal of Robotic System*. Vol. 11, No.6, 1994, pp.517-521.
- [14] V. Santibañez, R. Kelly, & F. Reyes, A new set-point controller with bounded torques for robot manipulators. *IEEE Transactions on Industrial Electronics*. Vol.45, No.1, 1998, pp.126-133.
- [15] A. Loria, E. Lefeber, & H. Nijmeijer, Global asymptotic stability of robot manipulators with linear PID and PI²D control. *Journal on Stability and Control: Theory and Applications SACTA*, Vol.3, No.2, 2000, pp.138-148.
- [16] F. Reyes, and A. Rosado, Polynomial family of PD-Type controllers for robot manipulators. *Control Engineering Practice, Elsevier Ed.* Vol.13, 2005, 2005, pp. 441-450.
- [17] M. W. Spong, & M. Vidyasagar, *Robot Dynamics and Control*. John Wiley and Sons, 1989. 1989).
- [18] D. Koditschek, Natural motion for robot arms. *Proceedings of the 1984 IEEE Conference on Decision and Control*. Las Vegas N, 1984, pp.733-735.
- [19] R. Ortega, and M. Spong, Adaptive Motion Control of Rigid Robots: a Tutorial. *Automatica*, Vol.25, No.6, 1989, pp.877-888.
- [20] F. Reyes, & R. Kelly, Experimental evaluation of identification schemes on a direct drive robot. *Robotica*, Cambridge University Press. Vol.15, 1997, pp.563-571.
- [21] L. L. Whitcomb, A. A. Rizzi, & D. E. Koditschek, Comparative experiments with a new adaptive controller for robot arms, *IEEE Transactions on Robotics and Automation*, Vol. 9, No. 1, 1993, pp.59-69.
- [22] B. De Jager, & J. Banens, Experimental evaluations of robot controllers. *Proceedings of the 33rd. Conference on Decision and Control*. Lake Buena Vista, Fl. U.S.A., 1994, pp.363-368.
- [23] H. Berghuis, H. Roebbers & H. Nijmeijer, Experimental comparison of parameter estimation methods in adaptive robot control, *Automatica*, Vol. 31, No. 9, 1995, pp.1275-1285.
- [24] A. Jaritz & M. Spong.(1996). An experimental comparison of robust control algorithms on a direct drive manipulator. *IEEE Transactions on Control Systems Technology*. Vol.4, No.6, 1996, pp.363-368.
- [25] D. Koditschek, Strict global Lyapunov function for mechanical systems. *Proceedings of the IEEE American Control Conference*. Atlanta GA. 1988, pp.1770-1775.
- [26] J. T. Wen, A unified perspective on robot control: the energy Lyapunov function approach. *International Journal Adaptive Control Signal Proceedings*. No 4, 1990, pp.487-500.
- [27] J. T. Wen, K. Delgado and D. Bayard. Lyapunov function-based control laws for revolute robot arms: tracking control, robustness, and adaptive control. *IEEE transactions on Automatic Control*, AC-37, 1992, pp.231-237.
- [28] P. Tomei, Adaptive PD Controller for robot manipulators, *IEEE Transactions on Robotics and Automation*, RA-7, 1991, pp.564-570.
- [29] T. Hu, and Z. Lin, Composite Quadratic Lyapunov functions for constrained control systems. *IEEE Transactions on Automatic Control*, Vol. 48, No.3, 2003, pp.440-450.
- [30] F. Mazenc, and D. Nesić. Strong Lyapunov functions for systems satisfying the conditions of LaSalle. *IEEE Transactions on Automatic Control* Vol. 49, No.6, 2004, pp.1026-1030.
- [31] J. Adamy, Implicit Lyapunov functions and isochrones of linear systems. *IEEE Transactions on Automatic Control*, Vol.50, No. 6, 2005, pp. 874-879.
- [32] S. G. Nersesov, and W. M. Haddad, On the stability and control of nonlinear dynamical systems via Vector Lyapunov Functions. *IEEE Transactions on Automatic Control*. Vol. 51, No.2, 2006, pp.203-215.
- [33] F. Mazenc and M Malisoff, Further constructions of Control-Lyapunov Functions and Stabilizing Feedbacks for Systems Satisfying the Jurdjevic-Quinn Conditions. *IEEE Transactions on Automatic Control*. Vol. 51, No.2, 2006, pp. 360-365.
- [34] B. Armstrong-Hoélouvy, *Control of Machines with Friction*. Kluwer Academic Publishers 1991.

- [35] J. Alvarez, R. Kelly, & I. Cervantes Semiglobal stability of saturated linear PID control for robot manipulators. *Automatica*, Vol. 39, No.6, 2003, pp. 989–995.
- [36] Y. Su, D. Sun, L. Ren, and J. K. Mills, Integration of Saturated PI Synchronous Control and PD Feedback for control of parallel manipulators. *IEEE Transactions on Robotics*. Vol. 22, No.1, 2006, pp.202-207.
- [37] M. Sun, S. S. Ge, and I. M. Y. Mareels. Adaptive Repetitive Learning Control of Robotic Manipulators Without The Requirement for Initial Repositioning. *IEEE Transactions on Robotics*. Vol. 22, No.3, 2006, pp.563-568.
- [38] E. Jarzebowska . Control oriented dynamic formulation for robotic systems with program constraints. *Robotica, Cambridge University Press* Vol.24, 2006, pp.61-73.
- [39] B. Paden, & R. Panja, Globally asymptotically stable PD+ controller for robot manipulator. *International Journal of Control*, Vol.47, No.6, 1988, pp.1697-1712.
- [40] R. Kelly, Regulation of manipulators in generic task space: An energy shaping plus damping injection approach. *IEEE Transactions on Robotics and Automation*. Vol 15, No.2, 1999, pp.381–386.
- [41] V. Santibañez, R. Kelly, & F. Reyes, Strict Lyapunov Functions for control of robot manipulators. *Automatica*, Vol.33, No.4, 1997, pp.675–682.
- [42] Guangyu Liu, Subhash Challa, & Longguang Yu, Revisit Controlled Lagrangians for Spherical Inverted Pendulum. *International Journal of Mathematics and Computers in simulation*, Issue 2, Vol. 1, pp.209 - 214, 2007.
- [43] P. Sanchez-Sanchez, F. Reyes-Cortes, A. Michua-Camarillo, J. Cid-Monjaraz BUAP & M. Arias-Estrada INAOE *Control and simulation of a robot of two degrees of freedom (Implementation of a new control algorithms)*. *International Journal of Mathematics and Computers in simulation* Issue 4, Vol. 1, pp. 356 - 361, 2007
- [44] P. Sánchez-Sánchez, F. Reyes-Cortés , *Position Controller through Pascals Cartesian Controllers* WSEAS Transactions on systems Issue 12, Vol. 4, pp. 2417, 2005